

Phase transitions and pressure effects in simple pyridinium salts

This article has been downloaded from IOPscience. Please scroll down to see the full text article.

2003 J. Phys.: Condens. Matter 15 5933

(<http://iopscience.iop.org/0953-8984/15/35/303>)

View [the table of contents for this issue](#), or go to the [journal homepage](#) for more

Download details:

IP Address: 171.66.16.125

The article was downloaded on 19/05/2010 at 15:07

Please note that [terms and conditions apply](#).

Phase transitions and pressure effects in simple pyridinium salts

Marek Szafrński and Izabela Szafraniak¹

Faculty of Physics, Adam Mickiewicz University, Umultowska 85, 61-614 Poznań, Poland

Received 31 May 2003

Published 22 August 2003

Online at stacks.iop.org/JPhysCM/15/5933

Abstract

Structural phase transitions in the pyridinium iodide $[\text{C}_5\text{NH}_6]^+\text{I}^-$ and bromide $[\text{C}_5\text{NH}_6]^+\text{Br}^-$ crystals were studied by calorimetry, volumetric dilatometry and dielectric methods. The pressure dependences of the transition temperatures were determined by dielectric constant and differential thermal analysis measurements under hydrostatic pressures of up to 1 GPa. Analysis of the experimental data indicated that the p - T phase diagrams of simple pyridinium salts could include tri-critical points in the pressure range above 1 GPa. The effect of external hydrostatic pressure is correlated with the chemical pressure that appears due to the change in the anionic radius. A new model of the phase transition is proposed that includes antiferroelectric order and six-fold disorder of the pyridinium cations, respectively, in the low- and high-temperature phases.

1. Introduction

The considerable recent interest in the pyridinium salts is a consequence of the discovery of the ferroelectric properties of pyridinium tetrafluoroborate [1]. The studies undertaken in the last decade have concentrated mainly on the search for new ferroelectric compounds and to date have yielded six new ferroelectric pyridinium crystals (see [2] and references therein). It is characteristic of these crystal structures that their anionic sublattices are built of tetrahedral or pseudo-tetrahedral units. The other common feature concerns the long-range ferroelectric order, which is driven by a slowing down of the relaxation of the ionic orientational degrees of freedom. However, the alignment of the permanent dipole moments of the pyridinium cations seems insufficient to explain the origin of spontaneous polarization [3]. The role of the tetrahedral anions in the ferroelectric–paraelectric phase transition, as well as the structural implications following the ordering processes, are still not clear but can be crucial to understanding the microscopic mechanism of ferroelectricity in this group of materials. Therefore further studies are indispensable, including those on non-ferroelectric compounds of the pyridinium salts family that can serve as model structures.

¹ Present address: Max Planck Institute of Microstructure Physics, Weinberg 2, 06120 Halle, Germany.

In this paper we discuss the results of calorimetric, dilatometric and dielectric studies of pyridinium iodide $[\text{C}_5\text{NH}_6]^+\text{I}^-$ (hereafter PyI) and pyridinium bromide $[\text{C}_5\text{NH}_6]^+\text{Br}^-$ (hereafter PyBr) at ambient and high hydrostatic pressure. By choosing simple pyridinium halogenates, the molecular degrees of freedom are reduced to those related exclusively to the pyridinium cation. The other advantage is the rhombohedral symmetry of their high-temperature phases [4, 5], similar to that observed in the paraelectric phases of ferroelectric pyridinium tetrafluoroborate, perchlorate and fluorosulfonate. The PyI and PyBr crystals undergo first-order phase transitions near 249 and 270 K, respectively [6–8]. The many studies by x-ray diffraction [4], ^1H NMR [6, 7, 9], dielectric spectroscopy [9], calorimetry [6, 8], and neutron [5, 10] and Raman [11] scattering provided valuable information on these transitions. However, the microscopic picture of the transition mechanism is still unclear due to the inconsistency in some experimental results. In particular, the data obtained by scanning [6] and adiabatic [8] calorimetry has led to distinct models of disordering of pyridinium cations in the high-temperature phase. These discrepancies further motivated us to undertake this study.

2. Experimental details

The PyI and PyBr salts were prepared by crystallization from aqueous stoichiometric solutions of the pyridinium base and hydroiodic/hydrobromic acid.

Differential scanning calorimetry (DSC) measurements were carried out on a Perkin-Elmer DCS-2 calorimeter in the temperature range from 160 to 290 K at different heating/cooling rates from 2 to 10 K min^{-1} .

The specific volume at ambient pressure was measured with a Netzsch TMA402 dilatometer in the temperature range from 170 to 300 K at a heating rate of 0.5 or 1 K min^{-1} . The influence of hydrostatic pressure on the specific volume of the crystal was examined by pressure–volume dilatometry using the self-made equipment [12]. The isobaric measurements were performed at a few pressures in the range 10–150 MPa, while the temperature was changed at a rate of 0.5 K min^{-1} . The isotherms were obtained at a few temperatures in the range 230–300 K, while the pressure was changed at a rate of 10 MPa min^{-1} . All high-pressure dilatometric measurements were carried out in a high-pressure cell filled with silicon oil (AK12500 from Wacker Chemie). Freezing of the oil limited the low-temperature measurements to about 230 K. The volumetric measurements were performed on polycrystalline samples that were pressed into cylinders of 5.8 mm in diameter and about 10 mm in length.

The temperature dependence of the complex dielectric permittivity was measured using a Hewlett-Packard 4192A impedance analyser at several frequencies in the range between 10 kHz and 10 MHz. The measuring ac electric field was about 5 V cm^{-1} . The samples were prepared in the form of thin pressed pellets with deposited golden electrodes.

The studies in the high-pressure range up to 1 GPa were performed by differential thermal analysis (DTA) [13] and dielectric methods. The samples were mounted in a beryllium–copper cell, which was then filled with compressed helium. The pressure was generated by a GCA-10 Unipress gas compressor. A manganin gauge served for pressure calibration to an accuracy of ± 2 MPa. The temperature was changed at a rate of 2–3 and 1 K min^{-1} in the DTA and dielectric measurements, respectively. The temperature of the sample was controlled inside the cell by a copper–constantan thermocouple to an accuracy of ± 0.05 K. The transition temperatures were determined on heating the samples as the onset of thermal or dielectric anomaly.

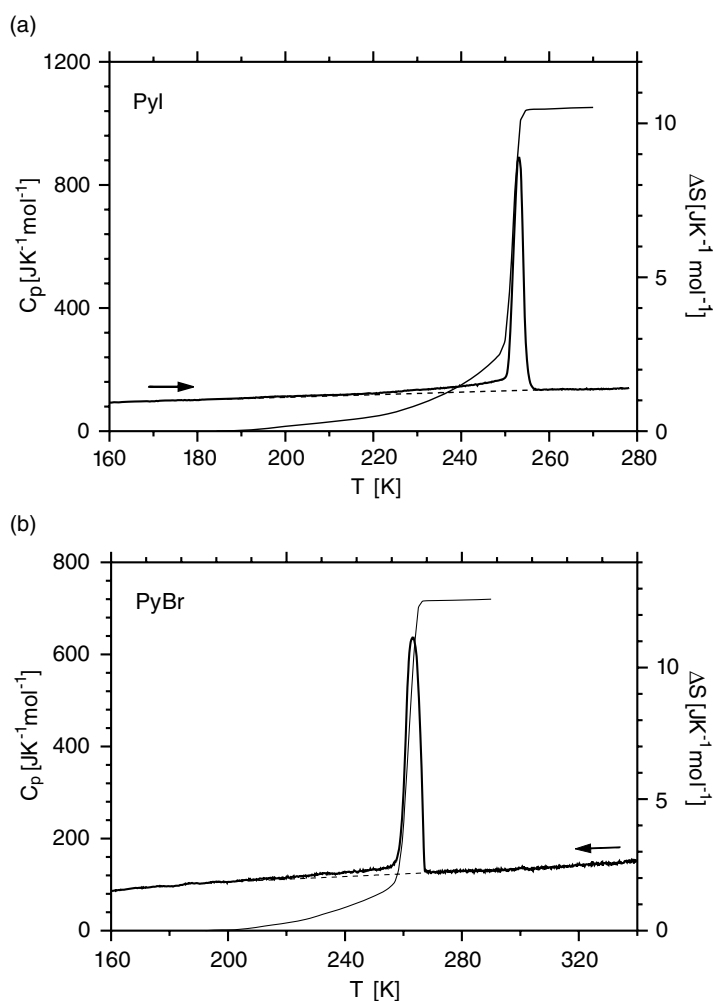


Figure 1. The temperature dependence of the specific heat C_p (thick solid curve) and the entropy change ΔS (thin solid curve) measured by the DSC method for (a) PyI and (b) PyBr. The dashed line marks the normal course of C_p ; the arrows indicate the cooling/heating runs.

3. Results

3.1. Thermal properties

The temperature dependences of the specific heat of PyI and PyBr were derived from the DSC measurements. Several DSC runs recorded at different rates of temperature change proved the very good repeatability of the results. Representative $C_p(T)$ curves are plotted in figure 1. The thermal anomalies are typical of the first-order phase transitions. Their character is further confirmed by the presence of thermal hysteresis, but it should also be stressed that the anomalous changes start several tens of degrees below the transition temperatures. The total entropy changes ΔS , including pre-transitional effects, were calculated by integrating the

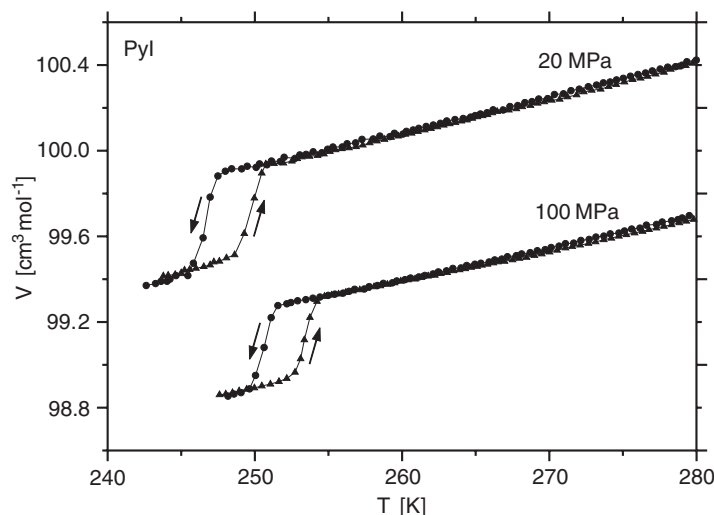


Figure 2. The temperature dependence of the specific volume of PyI in the vicinity of the transition temperature, measured at 20 and 100 MPa.

Table 1. The thermodynamic parameters of the phase transitions of PyI and PyBr.

	PyI	PyBr	References
T_0 (K)	246.8 ^a , 247.9 ^b	267.8 ^a , 271.6 ^b	This work
ΔS (J K ⁻¹ mol ⁻¹)	10.7 18.6–25.6 7.8	12.3 9.1	This work [8] [6]
ΔS_0 (J K ⁻¹ mol ⁻¹)	7.7	9.7	This work
ΔV (cm ³ mol ⁻¹)	0.41	0.8 ^c	This work

^a Cooling.

^b Heating.

^c Calculated from equation (6).

excess part of the specific heat according to the formula

$$\Delta S = \int \frac{C_p(T) - C_p^b(T)}{T} dT, \quad (1)$$

where $C_p^b(T)$ denotes the temperature dependence of the normal part of C_p , represented by the dashed curve in figure 1. Independently, the transition entropies ΔS_0 , corresponding to the transition enthalpies, were determined solely from the areas of the peaks. The values of ΔS and ΔS_0 are collected in table 1, together with the data from the literature.

3.2. Volumetric thermal expansion and compressibility

The dilatometric measurements of PyI revealed an increase in the crystal volume at T_0 when the sample was heated from the low- to the high-temperature phase. This characteristic of the first-order phase transition jump-wise change of the crystal volume, ΔV , is seen clearly in figure 2, showing the results of measurements at 20 and 100 MPa. At elevated pressures the anomaly was shifted towards higher temperatures. Simultaneously, the magnitude of ΔV decreased with increasing pressure. The pressure dependence of ΔV is plotted in

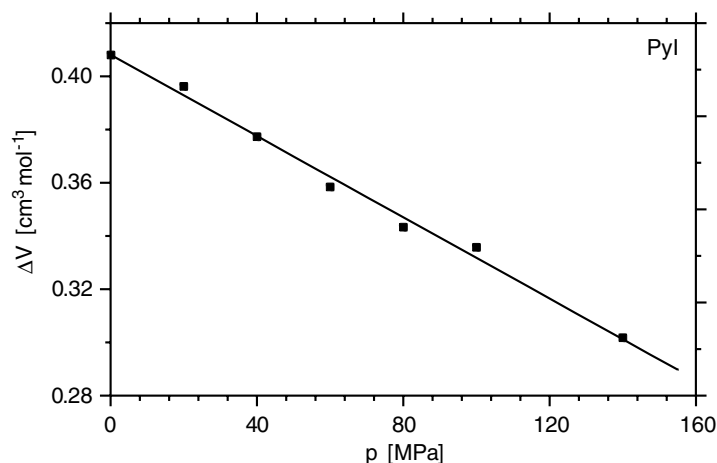


Figure 3. The pressure dependence of the volume change at the transition temperature in the pyridinium iodide crystal.

figure 3. The studies at ambient pressure proved that the volume expansion coefficient, $\alpha_V = 1/V(\partial V/\partial T)_p$, is similar in both phases of PyI. The values of α_V calculated for the low- and high-temperature phase amount to 2.6×10^{-4} and $2.7 \times 10^{-4} \text{ K}^{-1}$, respectively. The high-pressure isothermal measurements also allowed us to determine the coefficient of the crystal volume compressibility, $\beta = -1/V(\partial V/\partial p)_T$. In the high-temperature phase, $\beta = 1.5 \times 10^{-10} \text{ Pa}^{-1}$, which is close to the coefficient of $1.4 \times 10^{-10} \text{ Pa}^{-1}$ that is observed for both PyPF₆ [14] and PyBF₄ [15]. The almost identical compressibility of these compounds is a consequence of their very similar crystal structures.

3.3. Dielectric properties

The pyridinium salts are convenient objects for dielectric studies, since their structures contain permanent dipole moments associated with the cations. Therefore, any change in the cationic dynamics must modify the dielectric response of the crystal. This applies equally to the PyI and PyBr crystals, which exhibit profound changes in the dielectric constant at the phase transition temperatures. The temperature dependences of the real part of the complex dielectric permittivity $\epsilon'(T)$, measured on heating and cooling the polycrystalline samples at a frequency of 10 MHz, are shown in figure 4. In the high-temperature phases the dielectric constants of both crystals are quite high but differ in their magnitude and temperature behaviour. The dielectric increments observed at T_0 amount to as much as 7 and 18 units for PyI and PyBr, respectively. The difference in these values is significant, but both are large, indicating a sudden slowing down of the dipole motions when the crystals transform to the low-temperature phases. It is seen clearly that the pre-transitional effects, which are observed as a nonlinear increase in $\epsilon'(T)$ in the low-temperature phases, are much more pronounced in the iodide than in the bromide. It should also be mentioned that, at measuring field frequencies from 10 kHz to 13 MHz in the studied temperature range of 115 to 300 K, no dielectric relaxation process has been detected in the case of PyBr, while in PyI a weak dielectric absorption—similar to that described previously [9]—has been observed below 180 K. The difference in the dielectric responses of the iodide and bromide indicate that the dynamics of the cations evolve in various ways in these crystals. It is highly probable that in the bromide the cationic 60° reorientations are primarily triggered/frozen at T_0 , while in the iodide the transition changes in the frequency

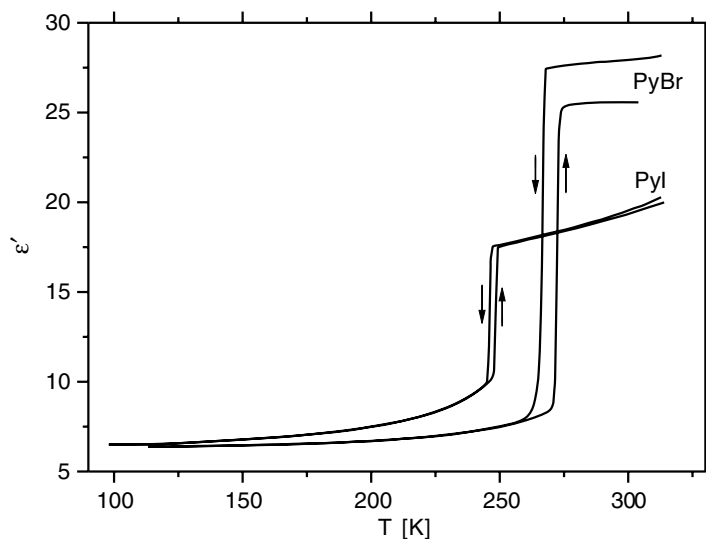


Figure 4. The real parts of the complex dielectric permittivity of PyI and PyBr, measured as a function of temperature at the electric field frequency of 10 MHz, on cooling and heating the samples, as indicated by the arrows.

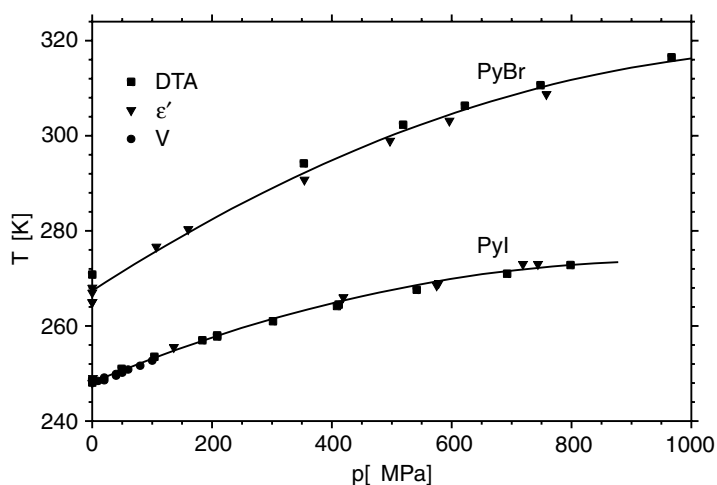


Figure 5. p - T phase diagrams of PyI and PyBr. The solid curves are the best fits to the experimental points using equations (2) and (3), respectively, for the iodide and the bromide.

of the cationic hopping are relatively smaller, in favour of a progressive thermally stimulated effect proceeding both below and above T_0 .

3.4. p - T phase diagrams

The results of earlier high-pressure dielectric studies of PyI [9] have been complemented by the present dilatometric and DTA measurements. As follows from figure 5, which shows the transition temperature versus pressure, the results obtained by different methods are consistent. In the pressure range studied, the data can be fitted well by a square polynomial function of

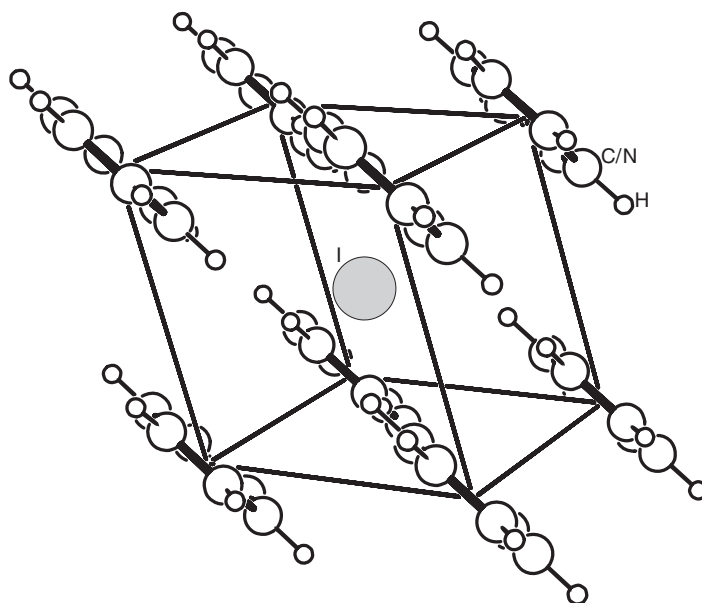


Figure 6. The high-temperature crystal structure of PyI, according to the data from [4], viewed perpendicular to the three-fold symmetry axis.

pressure:

$$T_0(p) = 248 \text{ (K)} + p \times 0.052 \text{ (K MPa}^{-1}\text{)} - p^2 \times 2.7 \times 10^{-5} \text{ (K MPa}^{-2}\text{)}. \quad (2)$$

The p - T phase diagram of the bromide (see figure 5) was determined on the basis of the high-pressure DTA and dielectric studies. The pressure dependence of the transition temperature is similar to that for PyI and can be described by an analogous pressure-dependent function:

$$T_0(p) = 266 \text{ (K)} + p \times 0.085 \text{ (K MPa}^{-1}\text{)} - p^2 \times 4.0 \times 10^{-5} \text{ (K MPa}^{-2}\text{)}. \quad (3)$$

4. Discussion

Simple pyridinium salts of the general formula PyX (where $X = \text{Cl}^-$, Br^- , I^- , PF_6^-) are characterized by isosymmetric high-temperature phases of space group $R\bar{3}m$. An exemplary crystal structure of such a type is shown in figure 6. The pyridinium cations are arranged in sheets perpendicular to one of the body diagonals of the rhombohedral unit cell. The cations are disordered around the three-fold symmetry axes, satisfying the symmetry of the crystal. The X ions are situated at the centre of the cells. The evident proximity of these crystal structures implies their similar properties. One of the common features is the first-order phase transition they undergo. The order-disorder mechanism of this transition has been discussed for many years [6–9, 14], but the problem still seems to be open. The latest model proposed for PyI by Hanaya *et al* [8] assumes a 12-position disordering in the high-temperature phase and a single-configuration order in the low-temperature phase. Unfortunately, this model—though based on precise calorimetric measurements—cannot be accepted for several reasons:

- (a) The low-temperature phase in such a case should be ferroelectric since, as a consequence of the single-configuration order, all the pyridinium dipoles should point in the same direction, resulting in a macroscopic spontaneous polarization of the crystal. Actually,

PyI does not exhibit ferroelectric properties in the low-temperature phase, similarly to the PyCl, PyBr and PyPF₆ crystals.

- (b) The model is inconsistent with the previous x-ray [4] and NMR [7] studies. The results of both these methods clearly indicate a six-fold disordering of the pyridinium ring in the high-temperature phase.
- (c) The excess entropy derived in [8] seems to be overvalued due to the unrealistic estimation of the normal part of $C_p(T)$. In particular, the contribution to the transition entropy accounted for by the integration of the $C_p(T)$ anomaly in a temperature range several dozen degrees above the transition temperature seems to be questionable and physically unjustified.

As shown in table 1, the total transition entropies obtained from the present DSC measurements of PyI and PyBr are much lower than those reported in [8]. Simultaneously, they are higher than the values of Ripmeester [6]. The latter are close to our values of ΔS_0 , which suggests that they do not include the pre-transitional contributions to ΔS . It should be stressed that the values of ΔS were measured with an uncertainty of $\pm 10\%$, which is much higher than the 2–3% accuracy of the calorimeter. This was caused by the fact that the temperature intervals of integration were relatively wide. Then a small change in the baseline approximating the normal part of $C_p(T)$ resulted in a significant change in ΔS . The total anomalous entropy change associated with an order–disorder phase transition includes the configurational (ΔS_C) and volumetric (ΔS_V) entropy changes. So, to obtain the configurational part, the volume-related component must be extracted from ΔS . Both contributions are not independent and, only to a first approximation, ΔS can be expressed as the sum

$$\Delta S = \Delta S_C + \Delta S_V. \quad (4)$$

The volumetric part can be estimated from the following formula [16, 17]:

$$\Delta S_V = \Delta V \frac{\alpha}{\beta}. \quad (5)$$

The value of ΔS_V calculated for PyI amounts to $0.75 \text{ J K}^{-1} \text{ mol}^{-1}$. For PyBr the volume change ΔV was not measured, but can be determined from the Clausius–Clapeyron equation:

$$\frac{dT_0}{dp} = \frac{\Delta V}{\Delta S_0}. \quad (6)$$

The calculations yield $\Delta V = 0.8 \text{ cm}^3 \text{ mol}^{-1}$. This value is twice as large as for PyI, which suggests that the volumetric contribution to the total entropy change in the bromide is much higher than in the iodide. This also explains the differences observed between the magnitudes of the thermodynamic parameters of both compounds (see table 1). Taking the ΔS_V contributions into account, the configurational parts ΔS_C can be reasonably estimated to be close to $R \ln 3$ (where R is a gas constant). This value can be compared to Boltzmann's formula:

$$\Delta S_C = R \ln \frac{N_1}{N_2}, \quad (7)$$

where N_1 and N_2 are the numbers of distinguishable configurations in the high- and low-temperature phases, respectively. It is highly probable that the low-temperature structures of the PyI and PyBr crystals are ordered with an antiferroelectric arrangement of cations, similarly to that observed in the low-temperature phase of PyCl [18]. In agreement with the antiferroelectric order, two configurations ($N_2 = 2$) must be assumed in the low-temperature phases of PyI and PyBr. Thus, according to equation (7), we arrive at $N_1 = 6$ configurations in the high-temperature phases. This result corroborates the model of the six-fold reorientations of the pyridinium ring in the high-temperature phase arising from the NMR [6, 7] and structural [4]

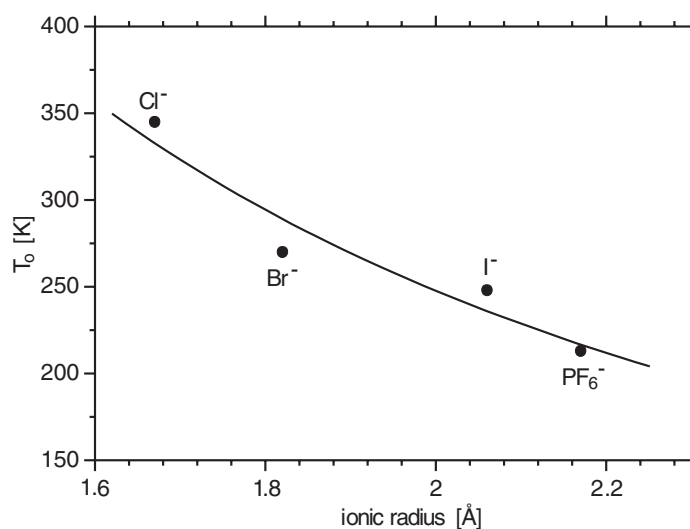


Figure 7. The correlation between the anionic radius and the transition temperature of the crystal. The ionic radii of the halogens were taken after Shannon [19]. For estimating the radius of PF_6^- we additionally used crystallographic data from [20].

studies, and also strongly supports the mechanism of the ferroelectric phase transition that was proposed recently for PyBF_4 [15]. In the latter case, the total entropy change associated with two successive, continuous phase transitions amounts to $18\text{--}24 \text{ J K}^{-1} \text{ mol}^{-1}$, depending on the estimation of the normal part of $C_p(T)$. This entropy gain—much higher than that observed for the non-ferroelectric PyX crystals (see table 1)—originates from an additional disorder of the BF_4^- anions, and is also a consequence of the ferroelectric (and thus single-configuration) order of the pyridinium cations in the low-temperature phase.

It is worth noting that, although the ordering of the cations at T_0 breaks the symmetry of the crystal, the structure is not perfectly ordered just below the transition point. The cationic dynamics slow down over a broad temperature range, as evidenced by the anomalous behaviour of the $\varepsilon'(T)$ and $C_p(T)$ dependences (see figures 1 and 4). This conclusion is also supported by the fact that the values of $\Delta S_0 - \Delta S_V$ are lower than $R \ln 3$.

It is interesting that the transition temperatures of the PyX crystals depend strongly on the kind of anion, in particular on its size. This dependence is illustrated in figure 7, showing a correlation between T_0 and the ionic radius. A decrease in the anionic radius leads to an increase in T_0 . When the size of the anion is reduced from PF_6^- to Cl^- the pyridinium sheets approach one another and the electrostatic interactions rise. Due to the antiferroelectric order in the low-temperature phase, the dipoles are arranged antiparallel and the process of bringing the cations closer together strengthens their coupling. Thus, higher energy is required for breaking this coupling and consequently the transition occurs at higher temperature. The tuning of the structural parameters of the crystal due to the radius of the anion can be regarded as the application of an internal chemical pressure. In this group of pyridinium salts the decrease in cationic size is a method of reducing the inter-sheet spacing, analogous to the application of an external pressure. Actually, at elevated hydrostatic pressures, the transition temperatures also shift upwards (see figure 5 and [14]). The boundaries between the phases of the PyI and PyBr crystals are evidently nonlinear. According to equation (6), this nonlinearity can arise from the pressure-induced changes of ΔV or/and ΔS_0 . To clarify this problem we

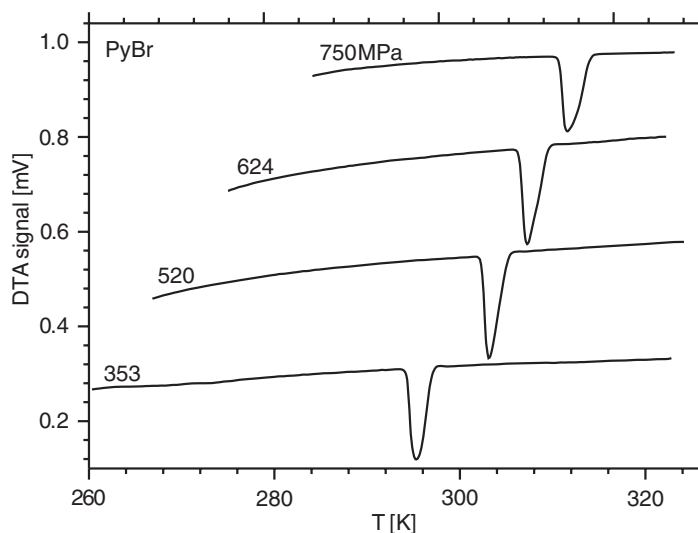


Figure 8. Exemplary DTA runs recorded on heating the PyBr sample at several pressures.

performed a careful analysis of our high-pressure calorimetric data. As in the pressure range below 300 MPa, the sensitivity of our set-up depends on the applied pressure [13]; only the runs recorded at higher pressures were taken into account. A comparison of the peak areas proved that, within experimental error, there was no change in the entropy due to the applied pressure either for PyI or PyBr. The exemplary DTA runs recorded on heating the PyBr sample at several pressures are shown in figure 8. Taking into consideration the results of our high-pressure dilatometric studies, we can conclude that the decrease in ΔV with pressure (see figure 3) is responsible for the nonlinear behaviour of the $T_0(p)$ dependences. Assuming that the pressure dependence of ΔV observed below 100 MPa for PyI is also satisfied at higher pressures, a simple extrapolation shows that, at about 1.3 GPa, the jump in the crystal volume should disappear. The absence of the volume change, which is characteristic of second-order phase transitions, indicates a possible tri-critical point on the transition line of PyI. A similar singularity can be expected for the bromide, probably at higher pressures.

Finally, we would like to point out that the pyridinium salts under study, apart from the obvious similarities, also exhibit diverse features. First of all, the character of the phase transition is different. The sharpness of the dielectric anomaly, the magnitudes of ΔV and ΔS_0 , and the temperature hysteresis of 3.8 K observed for the bromide indicate that the transition in this crystal is of first-order type, to a greater degree than that in the iodide. It is highly probable that the low-temperature structure of PyBr is better ordered just below T_0 compared to PyI, as is evident from the smaller pre-transitional effect seen clearly in figure 4. Although, by all appearances, these are slight differences, they can easily be discriminated under hydrostatic pressure. In figure 9 we re-plotted the p - T phase diagrams of PyI and PyBr together with the diagram of PyPF₆, scaling the temperature with respect to T_0 . It appears that the pressure effects in PyI and PyPF₆ are almost identical, which is consistent with the weakly first-order transitions observed in both these compounds. A distinctly different pressure dependence of the transition temperature of PyBr is a consequence of the much stronger first-order character of the transition in this case.

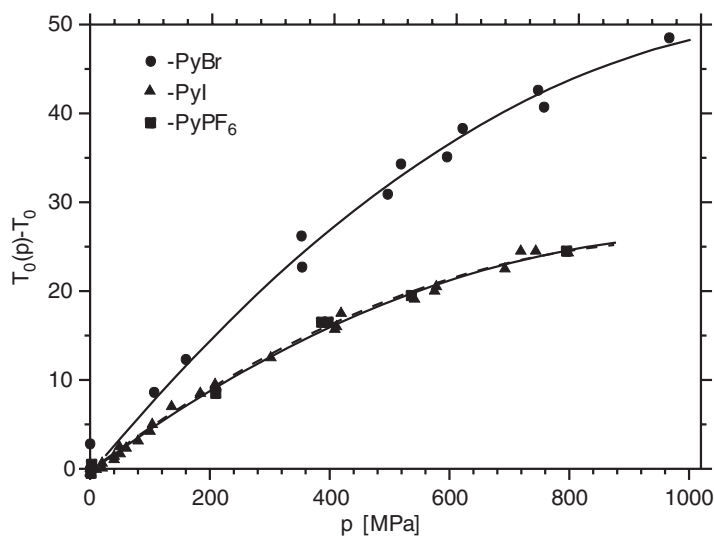


Figure 9. The p - T phase diagrams of PyI, PyBr and PyPF₆, scaled with respect to the transition temperatures at ambient pressure. The solid curves represent the best fits (similarly to those in figure 5); the dashed curve is the best fit to the experimental points of PyPF₆ [14].

5. Conclusions

The order–disorder phase transition in simple pyridinium salts can be described as a transition between the antiferroelectric and the paraelectric phases. Thus, at least two configurations that follow antiparallel coupling of the dipole moments characterize the low-temperature phase. Consequently, a six-fold dynamic disordering of the cations in the high-temperature phase ensures the disappearance of the net dipole moment of the pyridinium ring and explains the magnitude of the configurational entropy change associated with the transition.

For the ferroelectric pyridinium salts the picture is much more complex due to the additional disordering of the tetrahedral anions. Considering only the ferroelectric compounds with the same rhombohedral symmetry ($R\bar{3}m$) of the paraelectric phases as the symmetry of the high-temperature phases of the PyX derivatives, it is justifiable to assume the model of six-fold reorientation of the cation for the ferroelectric crystals too. It should be stressed that the entropy change that arises exclusively from the freezing of the cationic dynamics can be—depending on the kind of ferroelectric ordering—at most twice as large as in PyI or PyBr. However, taking these arguments into account and bearing in mind the disordering of the anion, it is impossible to reproduce reasonably the model that was proposed recently [21] for ferroelectric pyridinium tetrafluoroborate. The hundreds of distinguishable configurations, postulated for the description of the paraelectric phase of this compound, are characteristic rather of soft matter than of ionic crystals.

The results presented in this paper show the prominent role of the cation–cation interaction in the transition mechanism, which is reflected in the parallelism between the hydrostatic and chemical pressure, among others. The application of external pressure affects the transition temperature in a similar way to the application of chemical pressure. The latter is applied along the PyX series by reducing the radius of the X ion. The general analogy does not cover all specific features of the transition, such as its sharpness, which cannot be understood in terms of the cation–cation interplay alone.

Finally, we would like to point out that further studies of the PyX salts under higher pressures (above 1 GPa) are required to check the predicted change in character of the transition from first- to second-order.

Acknowledgments

One of the authors (IS) is grateful to Dr P U Mayr, Mrs A-M Saier and Dr G W Höhne of Ulm University for their help in dilatometric and calorimetric measurements, and to Dr P Czarnecki of the Adam Mickiewicz University for his assistance in part of the high-pressure measurements.

References

- [1] Czarnecki P, Nawrocik W, Pajak Z and Wasicki J 1994 *Phys. Rev. B* **49** 1511
- [2] Pajak Z, Maluszyńska H, Szafranska B and Czarnecki P 2002 *J. Chem. Phys.* **117** 5303
- [3] Pajak Z, Czarnecki P, Maluszyńska H, Szafranska B and Szafran M 2000 *J. Chem. Phys.* **113** 848
- [4] Hartl H 1975 *Acta Crystallogr. B* **31** 1781
- [5] Wasicki J, Nawrocik W, Pajak Z, Natkaniec I and Belushkin A V 1989 *Phys. Status Solidi a* **114** 497
- [6] Ripmeester J A 1976 *Can. J. Chem.* **54** 3453
- [7] Ripmeester J A 1986 *J. Chem. Phys.* **85** 747
- [8] Hanaya M, Ohta N and Oguni M 1993 *J. Phys. Chem. Solids* **54** 263
- [9] Lewicki S, Wasicki J, Czarnecki P, Szafraniak I, Kozak A and Pajak Z 1998 *Mol. Phys.* **94** 973
- [10] Mukhopadhyay R, Mitra S, Tsukushim I and Ikeda S 2001 *Chem. Phys. Lett.* **341** 45
- [11] Wong P T T and Ripmeester J A 1980 *Chem. Phys. Lett.* **72** 122
- [12] Dollhopf W, Barry S and Strauss M J 1991 *Frontiers of High-Pressure Research* ed H D Hochheimer and R D Ethers (New York: Plenum) pp 25–32
- [13] Szafranski M, Czarnecki P, Katrusiak A and Habrylo S 1992 *Solid State Commun.* **82** 277
- [14] Szafraniak I, Czarnecki P, Mayr P U and Dollhopf W 1999 *Phys. Status Solidi b* **213** 15
- [15] Szafraniak I, Czarnecki P and Mayr P U 2000 *J. Phys.: Condens. Matter* **12** 643
- [16] Orani R A 1953 *J. Chem. Phys.* **19** 93
- [17] Karasz F E, Couchman P R and Klempner D 1977 *Macromolecules* **10** 88
- [18] Rérat P C 1962 *Acta Crystallogr.* **15** 427
- [19] Shannon R D 1976 *Acta Crystallogr. A* **32** 751
- [20] Copeland R F, Conner S H and Meyers E A 1966 *J. Phys. Chem.* **70** 1288
- [21] Hanaya M, Shibasaki H, Oguni M, Nemoto T and Ohashi Y 2000 *J. Phys. Chem. Solids* **61** 651